Resonance Raman Spectroscopy of Met121Glu Azurin†

M. Adam Webb,‡ Cynthia N. Kiser,§ John H. Richards,§ Angel J. Di Bilio,§ Harry B. Gray,*,§ Jay R. Winkler,§ and Glen R. Loppnow*,‡

Department of Chemistry, University of Alberta, Edmonton, Alberta Canada T6G 2G2 and Beckman Institute, California Institute of Technology, Pasadena, California 91125

Received: March 2, 2000; In Final Form: September 11, 2000

The resonance Raman spectra for *Pseudomonas aeruginosa* Met121Glu azurin have been measured at wavelengths throughout the 600-nm absorption band at low and high pH. The spectra of the mutant at pH 3.5 and 7.0 are identical. Analysis of the 600-nm absorption band and resulting resonance Raman excitation profiles under both pH conditions indicates that the excited-state distortions in this mutant are smaller than those in the native protein.

Introduction

Blue copper proteins exhibit distinct spectroscopic and electrochemical properties that are attributable to constrained coordination in the β-barrel structure.[1−5] One of the best studied blue proteins, *Pseudomonas aeruginosa* azurin, has a single copper ion strongly ligated to one cysteine (Cys112) and two histidines (His46 and His117), with weakly ligated methionine (Met121) and glycine (Gly45) residues in an irregular trigonal bipyramidal coordination geometry (Figure 1A).[6,7] Work by Solomon and co-workers has shown that the characteristic 628-nm band in the azurin absorption spectrum is attributable to S(Cys-π) → Cu(x^2-y^2) charge transfer.[8] Other features in the 400−1000 nm region have been assigned to d−d, S(Met) → Cu, N(His) → Cu, and S(Cys-σ) → Cu transitions.[9−11]

There has been much discussion of the role of axial interactions in tuning the properties of blue copper proteins.[5,12−14] Absorption,[15,16] resonance Raman,[17] EPR,[18] and XAFS[19] spectroscopic studies all have suggested that the copper site structure in Met121Glu *P. aeruginosa* azurin at pH 7.0 is different from the structure at pH 4.0 or that in the wild-type protein. Apparently, deprotonation of the axial ligand (Glu121) strongly perturbs the copper coordination geometry (Figure 1B).[20] To examine this matter further, we have investigated the resonance Raman spectra of the Met121Glu mutant at pH 7.0 and 3.5. Surprisingly, we have found that the spectra of the mutant are similar at the two pH extremes for >600-nm excitation. Absorption features and excitation profiles can be interpreted in terms of smaller distortions in the excited states of the Met121Glu mutant at both pH 3.5 and 7.0 than those in the native protein.

Experimental Section

***Pseudomonas aeruginosa* Met121Glu Azurin.** The mutant was prepared and purified according to literature methods.[21,22]

Resonance Raman spectroscopy. Met121Glu azurin pH 7.0 samples were prepared by quantitative dilution of a stock solution (2.0−4.5 mM azurin, 100 mM sodium phosphate, pH 7.0) with a cacodylate/cacodylic acid buffer solution (2 M cacodylic acid, 100 mM sodium phosphate, pH 7.0); pH 3.5 samples were prepared by quantitative dilution of 0.83−1.0 mM azurin solution (15 mM sodium acetate, pH 3.5) with a sulfate/acetate solution (2 M Li_2SO_4, 15 mM sodium acetate, pH 3.5). The addition of cacodylate/cacodylic acid buffer or sulfate/acetate solutions did not have a noticeable effect on the absorption or resonance Raman spectra of the mutant.

Resonance Raman spectra of Met121Glu azurin at pH 7.0 were measured on solutions having an absorbance of 2.2−4.9 OD/cm at 597 nm (ϵ = 1100 $M^{-1}cm^{-1}$);[20] intensities due to the protein relative to the 605 + 638 cm^{-1} lines of cacodylate were measured by integration of peak areas. Correction for sample bleaching was done by measuring the absorbance at 500 nm (ϵ = 509 $M^{-1}cm^{-1}$) before and after each scan; the average absorbance was used to determine the azurin concentration. Measurements of the resonance Raman spectra of Met121Glu azurin at pH 7.0 were repeated on two fresh samples for each wavelength. Measurements at pH 3.5 were conducted on solutions having an absorbance of 3.75−4.55 OD/cm at 622 nm (ϵ = 4500 M^{-1} cm^{-1});[20] intensities of Met121Glu azurin relative to the 982 cm^{-1} line of sulfate were measured by integration of peak areas. The resonance Raman spectrum was insensitive to concentration for Met121Glu azurin at both pH 3.5 and 7.0. Correction for sample bleaching was done by measuring the absorbance at 560 nm (ϵ = 2170 $M^{-1}cm^{-1}$) before and after each scan, and the average absorbance was used to determine the azurin concentration. The sample volume was ∼200−300 μL in each case; the spectra were analyzed as described previously.[23−25] Wavelengths of 500 and 560 nm for Met121Glu azurin at pH 3.5 and 7.0, respectively, were chosen for monitoring sample bleaching rather than the 410 and 622 nm absorption maxima due to the high absorbance at these latter wavelengths. Measurements at wavelengths other than 500 and 560 nm yielded similar bleaching rates. Measurements of the resonance Raman spectra of Met121Glu azurin at pH 3.5 were only possible for one sample at each wavelength due to the limited amount of sample and irreversible photodecomposition observed at excitation wavelengths shorter than 600 nm.

The observed bleaching in an 80-minute scan was <5% at both pH 3.5 and 7.0 for the wavelengths used in the quantitative

† Part of the special issue "Thomas Spiro Festschrift". Dedicated to Professor Thomas G. Spiro on the occasion of his 65th birthday.

* To whom correspondence and reprint requests should be addressed.
‡ University of Alberta. E-mail: glen.loppnow@ualberta.ca
§ Beckman Institute, California Institute of Technology. E-mail: hgcm@its.caltech.edu.

10.1021/jp000832j CCC: $19.00
Published on Web 10/24/2000

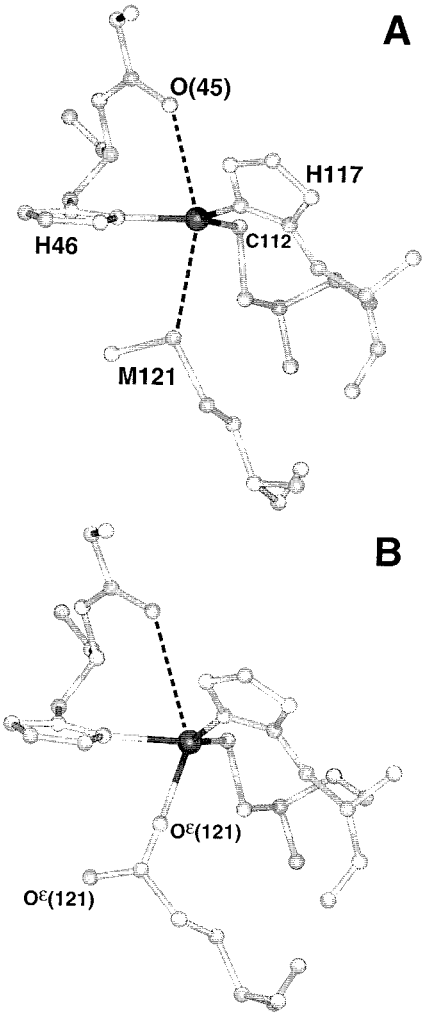

Figure 1. (A) Structure of the copper site of *P. aeruginosa* azurin. The broken lines indicate weak axial interactions of the copper atom with the S^{δ} of Met121, and the carbonyl oxygen of Gly45 (bond lengths $\sim$ 3 Å).[6,7] (B) Structure of the copper site of Met121Glu azurin: the Cu−O^{ϵ}(Glu121) bond length is 2.21 Å (average); the carbonyl oxygen (Gly45) to Cu average distance is 3.4 Å. The crystal structure was determined at a resolution of 2.3 Å using crystals grown at pH 6.0. It was estimated that in ~80% of the protein molecules Glu121 was protonated.[20]

analysis, suggesting that the bulk photoalteration parameter[26] is small. Absolute resonance Raman cross-sections of Met121Glu azurin were found from the relative integrated resonance Raman intensities.[23−26,27]

The absorption and resonance Raman cross-sections in the Condon approximation can be written using the time dependent formalism of Lee and Heller:[28,29]

$$\sigma_A = \frac{4\pi E_L e^2 M^2}{6\hbar^2 cn} \int_{-\infty}^{\infty} dE_0 H(E_0) \times \int_{-\infty}^{\infty} dt \langle i|i(t)\rangle \exp\left\{\frac{i(E_L + \epsilon_i)t}{\hbar}\right\} G(t) \quad (1)$$

$$\sigma_R = \frac{8\pi E_S^3 E_L e^4 M^4}{9\hbar^6 c^4} \int_{-\infty}^{\infty} dE_0 H(E_0) \times \left| \int_{0}^{\infty} dt \langle f|i(t)\rangle \exp\left\{\frac{i(E_L + e_i)t}{\hbar}\right\} G(t) \right|^2 \quad (2)$$

where E_L and E_S are the energies of the incident and scattered photons, respectively, n is the refractive index, M is the transition length, ϵ_i is the energy of the initial vibrational state, $|i\rangle$ and $|f\rangle$ are the initial and final vibrational wave functions, $H(E_0)$ is a normalized inhomogeneous distribution of site electronic energies (usually assumed to be Gaussian), $G(t)$ is the homogeneous line width function, and $|i(t)\rangle = e^{-iHt/\hbar}|i\rangle$ is the initial ground vibrational wave function propagated on the excited-state potential surface. Significantly, the $\langle i|i(t)\rangle$ and $\langle f|i(t)\rangle$ overlaps are only sensitive to Δ, the difference in ground- and excited-state equilibrium geometries along each normal mode, within the separable harmonic oscillator approximation. Thus, the resonance Raman intensities directly reflect the dynamics of the excited state. Implementation of these equations has been described in detail.[27,28] Analysis of the absorption spectrum and the resonance Raman excitation profiles of Met121Glu azurin was performed in the same manner as for other blue proteins.[23−25,30,31]

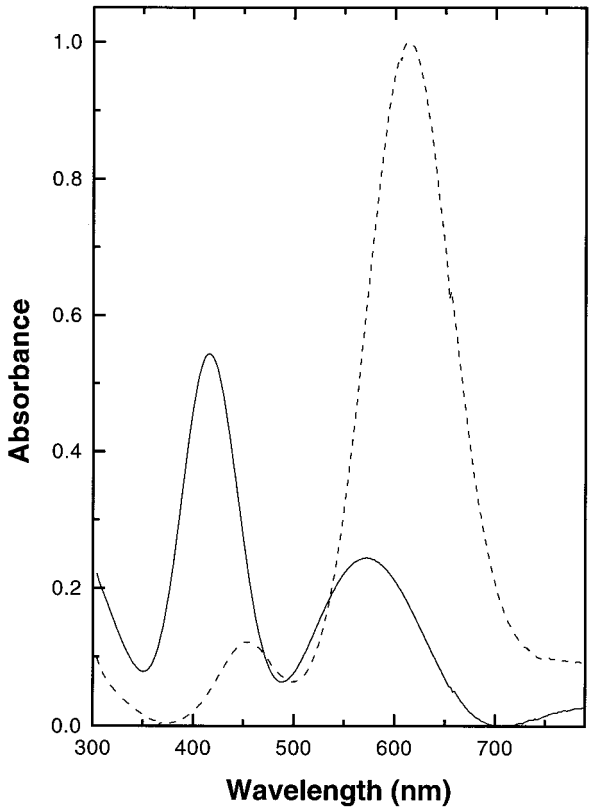

Figure 2. Absorption spectra of a 222 μM aqueous solution of *P. aeruginosa* Met121Glu azurin at pH 7.0 (solid line) and pH 3.5 (dashed line) at room temperature.

Results and Discussion

The absorption spectra of Met121Glu azurin at pH 3.5 and 7.0 are shown in Figure 2. The two-band pattern in these spectra is similar to that reported previously for the mutant at pH 4 and 8. The absorbance changes have been interpreted as arising from a pH-dependent equilibrium between two structures, a low pH form in which the protonated GluH is weakly ligated to the copper site through the carbonyl oxygen and a high pH form in which the deprotonated Glu is strongly ligated to the copper site through the carboxylate oxygen.[17,18,20]

The resonance Raman spectra of Met121Glu azurin at excitation wavelengths throughout the two-band system are shown in Figures 3 and 4. The sulfate and cacodylate vibrations (the intensity standards for pH 3.5 and 7.0, respectively) are at 982 (sulfate) and 606, 638 cm^{-1} (cacodylate). Sulfate was used

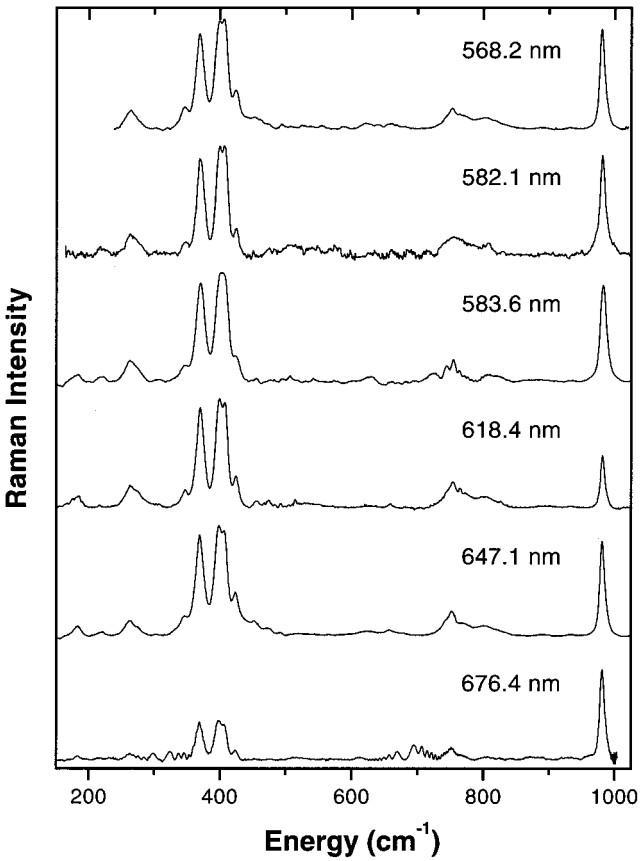

Figure 3. Resonance Raman spectra of *P. aeruginosa* Met121Glu azurin (pH 3.5), room temperature at excitation wavelengths throughout the 600-nm absorption band. Typical concentrations were 0.9 mM azurin and 500 mM sulfate. The spectra are the sum of three to nine scans and have been divided by a tungsten−halogen lamp spectrum (Eppley Laboratory, Inc.). The intensity standard (sulfate) appears at 982 cm^{-1}. All of the vibrational modes between 261 and 424 cm^{-1} were used in the analysis.

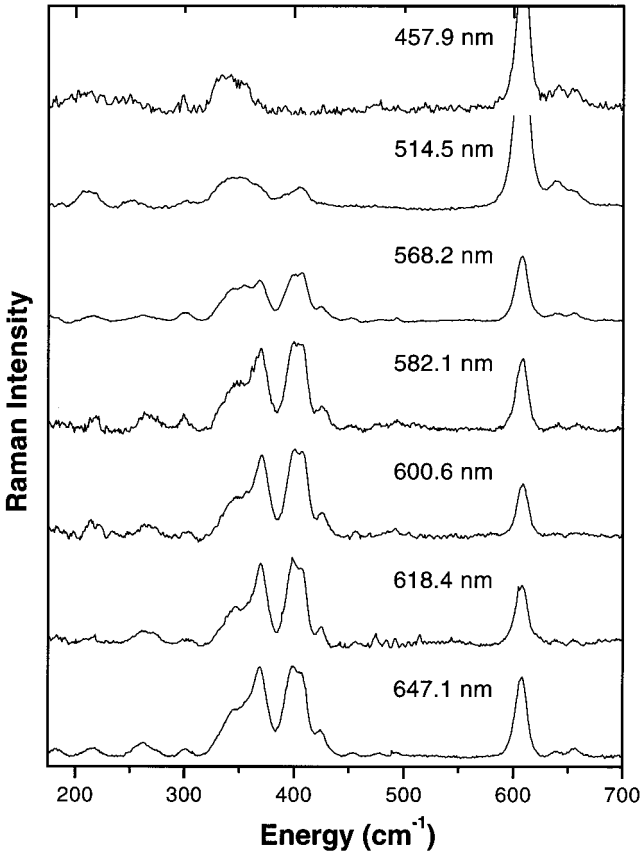

Figure 4. Resonance Raman spectra of *P. aeruginosa* Met121Glu azurin (pH 7.0), room temperature at excitation wavelengths throughout the 413- and 600-nm absorption bands. Typical concentrations were 3.3 mM azurin and 500 mM cacodylate. The spectra are the sum of three to nine scans and have been divided by a tungsten−halogen lamp spectrum (Eppley Laboratory, Inc.). The intensity standard (cacodylate) exhibits two bands, one at 605 and one at 638 cm^{-1}. All of the vibrational modes between 263 and 425 cm^{-1} were used in the analysis.

for the experiments at pH 7.0 because the mutant was more stable in sulfate than in cacodylate. The resonance Raman bands for azurin have been assigned previously.[17,32,33] Interestingly, the resonance Raman spectrum of the mutant at either pH is different from the spectrum of wild-type azurin[23] under identical conditions, suggesting some perturbation in the coordination geometry, electronic structure, or both (vide infra). The intensities of the azurin vibrations at both pH 3.5 and 7.0 relative to the intensities of the sulfate or cacodylate standard vibrations vary smoothly as a function of the excitation wavelength, as expected from the resonance enhancement effect.[28] However, the relative intensities of different vibrational modes of the protein vary differently with excitation wavelength, depending on the particular pH condition. At pH 3.5 (Figure 3), the resonance Raman spectra of Met121Glu azurin at all excitation wavelengths are similar, with only very slight relative intensity changes in the 396 and 407 cm^{-1} bands as the excitation wavelength is tuned from 568.2 to 618.4 nm. These two observations indicate that the observed modes are coupled to a single electronic transition in the mutant at pH 3.5. The resonance Raman spectra reported here at pH 3.5 also are identical with those reported previously at low temperature.[17,18]

The perturbed electronic structure of the copper site in Met121Glu azurin at pH 7.0 is reflected in the resonance Raman spectra, which evolve as the excitation wavelength is varied from 457.9 nm to ∼590 nm. At excitation wavelengths greater than 590 nm, the spectra are all similar. With excitation wavelengths between 457.9 and 582 nm, the spectrum evolves from one with a broad band at 345 cm^{-1} to one similar to that observed at pH 3.5, suggesting that the electronic state responsible for resonance enhancement of the Raman vibrations changes upon tuning from the 413-nm to the 600-nm absorption band. As expected, pre-resonance with the strong electronic transition at 410 nm is still observed in the spectra excited at longer wavelengths, as evidenced by the broad shoulder at 345 cm^{-1} in the spectra excited from 582 to 647 nm. The spectrum at 457.9 nm is similar, albeit with lower signal-to-noise qualities, to the one obtained in a low-temperature resonance Raman study of this species.[17,18] The lower signal-to-noise in the spectrum here results from photodecomposition at room temperature with excitation at 457.9 nm, not reported in the low-temperature study. The rate of photodecomposition decreased steadily as the excitation wavelength was tuned to longer wavelengths. Raman bands ca. 350 cm^{-1} observed for 457.9 nm excitation are still present at excitation wavelengths of 582.1 nm and higher with greater intensities than those in spectra at pH 3.5.

There is reasonably good agreement between the experimental and calculated absorption and resonance Raman excitation profiles (Figures 5 and 6, respectively). Similarities in the relative intensities at different excitation wavelengths indicate that the excitation profiles of these modes should be similar, and this is borne out in the calculations. At each pH, deviations of the experimental absorption spectrum from the calculated spectrum at both higher and lower energies are probably due to the presence of other transitions that were not modeled (vide

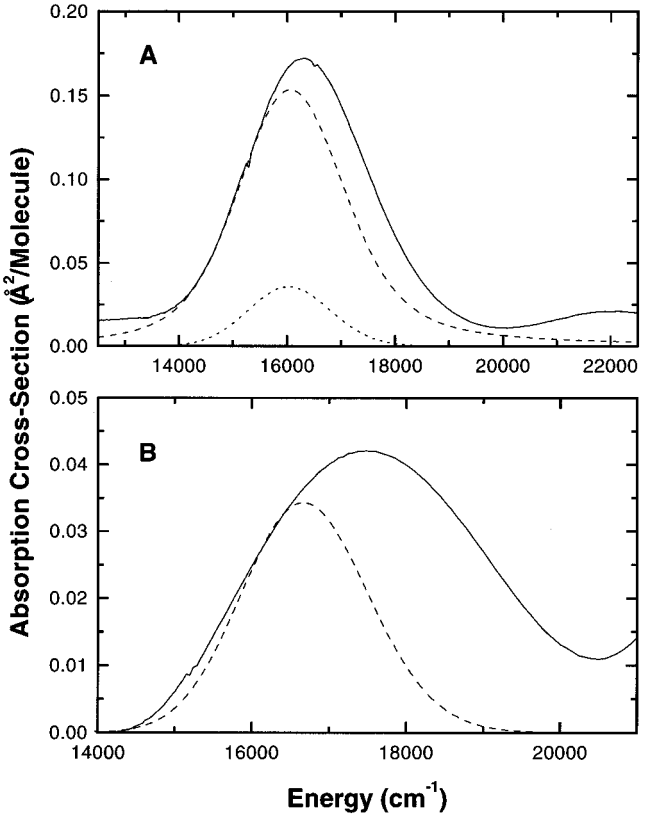

Figure 5. Experimental (solid line) and calculated (dashed line) absorption spectrum of azurin at pH 3.5 (A) and 7.0 (B). The dotted line in (A) is the calculated absorption spectrum using the alternative model (see text). The dashed and dotted lines are generated from eq 1 by using the parameters of Table 1. Deviations of the calculated from the experimental absorption spectrum at higher and lower energies arise from other electronic transitions that were not modeled and that contribute no resonance enhancement to the observed resonance Raman spectra.

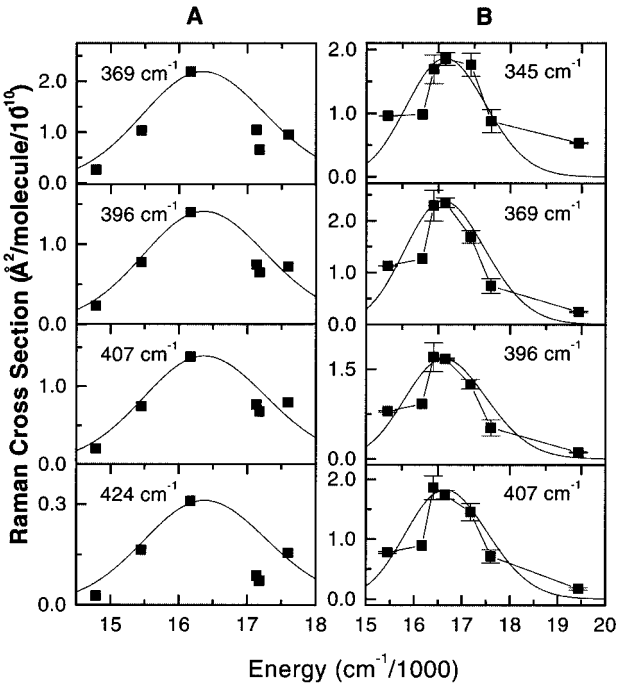

Figure 6. Experimental (points) and calculated (solid line) resonance Raman excitation profiles of the four most intense vibrational modes of azurin at pH 3.5 (A) and 7.0 (B). The excitation profiles were calculated with eq 2 by using the parameters of Table 1. Error bars represent the uncertainties in the absolute resonance Raman cross-sections at pH 7.0; no error bars are presented for the cross-sections at pH 3.5 as only one measurement was possible for each excitation wavelength.

infra). These deviations are particularly apparent in the pH 7.0 absorption spectrum and probably arise from tailing of the electronic transitions within the ca. 400-nm absorption band. Although the calculated resonance Raman excitation profiles are in fairly good agreement with experiment, the experimental excitation profiles are narrower than the absorption spectra at both pH 3.5 and 7.0, suggesting that more than one allowed electronic transition falls in the 597-nm region. The lack of resonance enhancement of specific modes by these other transitions, however, indicates that they have low oscillator strengths and/or minimal excited-state distortions.

The presence of additional transitions made it particularly difficult to model the absorption spectrum and resonance Raman excitation profiles of the mutant at pH 3.5. The resonance Raman cross-sections at both pH 3.5 and 7.0 are 4−14 times smaller than for the wild-type protein at all excitation wavelengths (Table 2). These small cross-sections are consistent with a lower transition oscillator strength, as observed in the mutant at pH 7.0. With minor variations of the line shape function, similar homogeneous and inhomogeneous broadening parameters can be used to model the absorption spectrum and resonance Raman excitation profiles of either the wild-type or mutant azurin at pH 7.0, albeit with very different excited-state displacements and electronic parameters. However, the small resonance Raman cross-sections are inconsistent with the wild-type-like transition oscillator strength found for the mutant at pH 3.5. As can be seen from Table 1, the homogeneous line width had to be significantly increased to obtain a reasonable fit to both the absorption spectrum and resonance Raman excitation profiles. Such a large increase in these parameters is difficult to justify physically, and arises primarily from assuming that most of the 600-nm absorption is due to this electronic transition. As an alternative, the parameters were re-optimized under the assumption that the homogeneous and inhomogeneous line widths are similar for the mutant at any pH (Figure 5A; Table 1). Under this assumption, the electronic transition responsible for resonance enhancement of the observed Raman vibrational modes becomes a much smaller component of the absorption band, comparable to the situation at pH 7.0.

To test this alternative model, the overtone and combination band intensities were measured for Met121Glu azurin at pH 3.5. The total Raman cross-section of the overtones and combination bands, summed over all of the bands between 700 and 850 cm^{-1}, is 1.19×10^{-11} Å^2/molecule at 568 nm and 2.83×10^{-11} Å^2/molecule at 647 nm. Calculating the overtone and combination band cross-sections using the standard model yields values of 6.71×10^{-13} and 3.14×10^{-12} Å^2/molecule at 568 and 647 nm, respectively, an order of magnitude lower than the experimental values. However, using the alternative model, calculated values of 1.02×10^{-11} and 3.76×10^{-11} Å^2/molecule are obtained at 568 and 647 nm, respectively, similar to the experimental values. This additional constraint provides further support for a perturbed electronic structure in the Met121Glu mutant under both pH conditions.

An alternative explanation for the evolution of the resonance Raman spectrum of Met121Glu azurin at pH 7.0 as the wavelength is tuned to long wavelengths is the presence of residual amounts of the pH 3.5 form of the mutant protein. Indeed, earlier measurements of the Raman intensities suggested that the inherent scattering from the pH 3.5 form is ∼7 times stronger than from the pH 7.0 form, although the respective

TABLE 1: Resonance Raman Parameters for *P. aeruginosa* Azurins

		Met121Glu	
parameter[a]	wild-type[b]	pH 3.5	pH 7.0
mode (cm^{-1}/unitless)	216/0.85	261/0.34 (0.34)	263/0.24
	263/1.26	275/0.36 (0.36)	300/0.16
	344/0.75	345/0.18 (0.18)	345/0.71
	371/1.60	369/0.66 (0.66)	355/0.23
	401/1.22	396/0.49 (0.49)	369/0.86
	408/1.64	407/0.48 (0.48)	396/0.71
	426/1.26	424/0.22 (0.22)	407/0.72
	439/0.23		425/0.36
	454/0.31		
	476/0.27		
	493/0.13		
	654/0.18		
E (cm^{-1})	2100	220 (220)	480
Γ_L (cm^{-1})	160	500 (0)	0
Γ_G (cm^{-1})	0	330 (100)	50
Θ (cm^{-1})	280	520 (650)	700
M (Å)	0.63	0.63 (0.24)	0.24
ν_{max} (cm^{-1})	16000	16200 (16200)	17500
LMCT (cm^{-1})	16200	16000 (16000)	16600
E_{00} (cm^{-1})	14200	15800 (15800)	16200

[a] Mode is the mode frequency (in cm^{-1})/Δ (in units of dimensionless normal coordinates), $E = \Sigma(\Delta^2\nu/2)$, Γ_L is the Lorentzian homogeneous line width, Γ_G is the Gaussian homogeneous line width, Θ is the Gaussian inhomogeneous line width, M is the transition length, ν_{max} is the absorption maximum, LMCT is the absorption maximum of the S $\rightarrow$ Cu LMCT electronic transition, and E_{00} is the zero-zero electronic energy. The values for Δ, E, Γ_L, Γ_G, Θ, M, LMCT, and E_{00} were obtained from simulations of the absorption spectrum and resonance Raman excitation profiles shown in Figures 5 and 6. The values in parentheses in the Met121Glu pH 3.5 column are for the alternative model (see text). [b] Values taken from ref 23.

TABLE 2: Summed Resonance Raman Cross-Sections for *P. aeruginosa* Azurins[a]

		Met121Glu	
λ	wild-type[b]	pH 3.5	pH 7.0
568	22.2	2.90	3.38
582	32.0	2.35	7.16
618	42.2	6.08	4.67
647	27.8	2.99	4.23

[a] In this table, λ is the excitation wavelength in nm and the total cross-sections are in units of $Å^2$/molecule $\times 10^{10}$. The errors in the total cross-sections are estimated to be $\pm$15%. The cross-sections are summed over all of the fundamental vibrational modes observed between 200 and 700 cm^{-1}. [b] Values taken from ref 23.

excitation wavelengths were not reported.[17] As a check, we calculated the Raman cross-sections for Met121Glu azurin at pH 7.0 assuming all of the observed resonance Raman scattering arises from residual pH 3.5 Met121Glu azurin. To be consistent with the absorption spectrum at pH 7.0, the calculated concentration of Raman-active species must be 10 times lower under this assumption, because the extinction coefficient is $\sim$10 times larger for the pH 3.5 form. However, the observed Raman intensity is also dependent on concentration, and the concentration must be divided from the observed intensity to yield the Raman cross-section. Thus, the assumption that all of the resonance Raman scattering observed with excitation wavelengths >600 nm arises from a residual amount of the pH 3.5 form of the mutant protein yields cross-sections that are an order of magnitude larger than from the same form of the protein at the same excitation wavelength. Given that our error estimates are on the order of 25%, this assumption is not in accord with the experimental absorption and resonance Raman intensities.

Concluding Remarks

Both the high and low pH forms of the M121E azurin mutant display substantially smaller resonance Raman cross-sections than the wild-type protein. Previous studies have suggested that this is a characteristic property of rhombic type 1 copper sites.[17] Our analysis attributes this effect to less distorted excited states in the mutant protein (Table 1), an interpretation that contrasts with experimental evidence that the electron-transfer reorganization energy of M121E is actually somewhat larger than that of native azurin.[34] Reconciliation of this apparent discrepancy between excited-state distortions and electron-transfer reorganization energy will require further investigation.

Acknowledgment. Work at the University of Alberta was supported by NSERC; work at Caltech was supported by NIH DK19038.

References and Notes

(1) Adman, E. T. In *Advances in Protein Chemistry*, Anfinsen, C. B., Richards, F. M., Edsall, J. I., Eisenberg, D. S., Eds.; Academic Press: San Diego, 1991, 145−198.

(2) Williams, R. J. P. *Eur. J. Biochem.* **1995**, *234*, 363.

(3) Winkler, J. R.; Wittung-Stafshede, P.; Leckner, J.; Malmström, B. G.; Gray, H. B. *Proc. Natl. Acad. Sci. U.S.A.* **1997**, *94*, 4246.

(4) Wittung-Stafshede, P.; Hill, M. G.; Gomez, E.; Di Bilio, A. J.; Karlsson, B. G.; Leckner, J.; Winkler, J. R.; Gray, H. B.; Malmström, B. G. *JBIC* **1998**, *3*, 367.

(5) Gray, H. B.; Malmström, B. G.; Williams, R. J. P. *JBIC* **2000**, in press.

(6) Nar, H.; Messerschmidt, A.; Huber, R.; van de Kamp, M.; Canters, G. W. *J. Mol. Biol.* **1991**, *218*, 427.

(7) Nar, H.; Messerschmidt, A.; Huber, R.; van de Kamp, M.; Canters, G. W. *J. Mol. Biol.* **1991**, *221*, 765.

(8) Penfield, K. W.; Gewirth, A. A.; Solomon, E. I. *J. Am. Chem. Soc.* **1985**, *107*, 4519.

(9) Solomon, E. I.; Penfield, K. W.; Gewirth, A. A.; Lowery, M. D.; Shadle, S. E.; Guckert, J. A.; Lacroix, L. B. *Inorg. Chim. Acta* **1996**, *243*, 67.

(10) Larsson, S.; Broo, A.; Sjölin, L. *J. Phys. Chem.* **1995**, *99*, 4860.

(11) Pierloot, K.; De Kerpel, J. O. A.; Ryde, U.; Roos, B. O. *J. Am. Chem. Soc.* **1997**, *119*, 218.

(12) De Kerpel, J. O. A.; Pierloot, K.; Ryde, U.; Roos, B. O. *J. Phys. Chem. B* **1998**, *102*, 4638.

(13) Malmström, B. G.; Leckner, J. *Curr. Opin. Chem. Biol.* **1998**, *2*, 286.

(14) Palmer, A. E.; Randall, D. W.; Xu, F.; Solomon, E. I. *J. Am. Chem. Soc.* **1999**, *121*, 7138.

(15) Karlsson, B. G.; Nordling, M.; Pascher, T.; Tsai, L.-C.; Sjolin, L.; Lundberg, L. G. *Protein Eng.* **1991**, *4*, 343.

(16) Di Bilio, A. J.; Chang, T. K.; Malmström, B. G.; Gray, H. B.; Karlsson, B. G.; Nordling, M.; Pascher, T.; Lundberg, L. G. *Inorg. Chim. Acta* **1992**, *198−200*, 145.

(17) Andrew, C. R.; Yeom, H.; Valentine, J. S.; Karlsson, B. G.; Bonander, N.; van Pouderoyen, G.; Canters, G. W.; Loehr, T. M.; Sanders-Loehr, J. *J. Am. Chem. Soc.* **1994**, *116*, 11489.

(18) Han, J.; Adman, E. T.; Beppu, T.; Codd, R.; Freeman, H. C.; Huq, L.; Loehr, T. M.; Sanders-Loehr, J. *Biochemistry* **1991**, *30*, 10904.

(19) Strange, R. W.; Murphy, L. M.; Karlsson, B. G.; Reinhammar, B.; Hasnain, S. S. *Biochemistry* **1996**, *35*, 16391.

(20) Karlsson, B. G.; Tsai, L.-C.; Nar, H.; Sanders-Loehr, J.; Bonander, N.; Langer, V.; Sjölin, L. *Biochemistry* **1997**, *36*, 4089.

(21) Piccioli, M.; Luchinat, C.; Mizoguchi, T. J.; Ramirez, B. R.; Gray, H. B.; Richards, J. H. *Inorg. Chem.* **1995**, *34*, 737.

(22) Faham, S.; Day, M. W.; Connick, W. B.; Crane, B. R.; Di Bilio, A. J.; Schaefer, W. P.; Rees, D. R.; Gray, H. B. *Acta Crystallogr.* **1999**, *D55*, 379.

(23) Webb, M. A.; Kwong, C. M.; Loppnow, G. R. *J. Phys. Chem. B* **1997**, *101*, 5062.

(24) Webb, M. A.; Loppnow, G. R. *J. Phys. Chem. B* **1998**, *102*, 8923.

(25) Webb, M. A.; Loppnow, G. R. *J. Phys. Chem. A* **1999**, *103*, 6283.
(26) Mathies, R. A.; Oseroff, A. R.; Stryer, L. *Proc. Natl. Acad. Sci. U.S.A.* **1976**, *73*, 1.
(27) Loppnow, G. R.; Mathies, R. A. *Biophys. J.* **1988**, *54*, 35.
(28) Myers, A. B.; Mathies, R. A. In *Biological Applications of Raman Spectroscopy*, Spiro, T. G., Ed.; Wiley: New York, 1988; Vol. 2, p 1.
(29) Lee, S.-Y.; Heller, E. J. *J. Chem. Phys.* **1979**, *71*, 4777.
(30) Fraga, E.; Webb, M. A.; Loppnow, G. R. *J. Phys. Chem.* **1996**, *100*, 3278.
(31) Loppnow, G. R.; Fraga, E. *J. Am. Chem. Soc.* **1997**, *119*, 896.
(32) Blair, D. F.; Campbell, G. W.; Schoonover, J. R.; Chan, S. I.; Gray, H. B.; Malmström, B. G.; Pecht, I.; Swanson, B. I.; Woodruff, W. H.; Cho, W. K.; English, A. M.; Fry, H. A.; Lum, V.; Norton, K. A. *J. Am. Chem. Soc.* **1985**, *107*, 5755.
(33) Woodruff, W. H.; Dyer, R. B.; Schoonover, J. R. In *Biological Applications of Raman Spectroscopy*, Spiro, T. G., Ed.; Wiley: New York, 1988; Vol. 3, p 413.
(34) Kiser, C. K. Ph.D. Thesis, California Institute of Technology, 1998.